

Precision measurements with highly charged ions at rest: The HITRAP project at GSI

F. Herfurth*, Th. Beier, L. Dahl, S. Eliseev, S. Heinz, O. Kester,
C. Kozhuharov, G. Maero, W. Quint

The HITRAP collaboration

Gesellschaft für Schwerionenforschung mbH, Planckstraße 1, 64291 Darmstadt, Germany

Received 19 December 2005; received in revised form 31 January 2006; accepted 6 February 2006

Available online 24 March 2006

Dedicated to H.-J. Kluge on the occasion of his 65th birthday.

Abstract

A decelerator will be installed at GSI in order to provide and study bare heavy nuclei or heavy nuclei with only few electrons at very low energies or almost at rest. Stripping at relativistic energies will produce highly charged ions. After electron cooling and deceleration in the experimental storage ring the ions are extracted from the storage ring at 4 MeV/u and further decelerated in a combination of an IH and four-rod RFQ structure. Finally, they are injected into a Penning trap where the ions are cooled to 4 K. From this cooler trap, the ions can be transferred in a quasi-continuous or pulsed mode to different experimental setups. High-precision measurements of electronic and nuclear binding energies will be performed in a Penning trap exploring the high charge states. Other key experiments focus on g -factor measurements of the bound electron, precision laser and X-ray spectroscopy, studies of ionic structure, hollow atoms, and ion-surface interaction at very low impact energies.

© 2006 Elsevier B.V. All rights reserved.

PACS: 07.75.+h Mass spectrometers; 21.10.Dr Binding energies and masses

Keywords: Atomic mass; Binding energy; Penning trap; Electron mass; g -Factor

1. Introduction

The theory of quantum electrodynamics delivers some of the most precise predictions in physics. For instance, it is able to predict with remarkable precision atomic level energies in the hydrogen atom [1]. This is achieved by a good understanding of perturbation theory. But, in very high electromagnetic fields, as they exist for instance in heavy, highly charged ions (HCI), it is no longer possible to perform calculations by perturbation theory in $Z\alpha$ since $Z \approx 1/\alpha$. Hence, a number of new techniques are required especially for QED calculations [2]. Additionally, effects like the nuclear size effect, or the charge distribution in the nucleus start to get big enough to play a role within the precision that can be reached today [2].

Experimentally, such high fields become accessible by stripping heavy atoms off all or most of their electrons. There are two approaches: stripping of the projectile at high energy or collisions with energetic electrons in an ion source. If moderately charged ions are accelerated and sent through a target, they will lose all or most electrons in collisions with the target atoms if the ion energy is high enough. Similarly, atoms placed in an electron beam will be stripped sequentially off their electrons, if the energy of the electrons in the beam and the electron beam current density are high enough. Both approaches have been used to produce heavy, highly charged ions (HCI) [3,4]. However, the most intense source of bare, heavy HCI as for instance U^{92+} ions is at GSI in Darmstadt, where the high-energy stripping approach is used.

For precision experiments a well-defined source of HCI is urgently needed. In the experimental storage ring (ESR) at GSI [5] the beam of HCI is cooled using electron cooling. Thus, the momentum and spatial position of the ion beam is defined with high

* Corresponding author. Tel.: +49 6159 71 1360; fax: +49 6159 71 2901.
E-mail address: F.Herfurth@gsi.de (F. Herfurth).

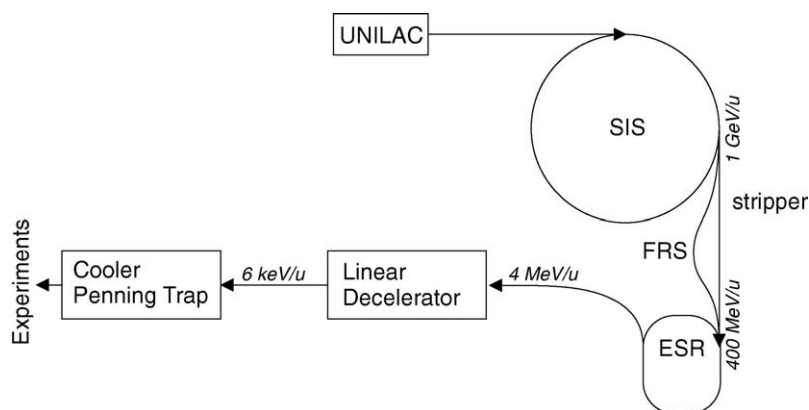


Fig. 1. Overview of the planned HITRAP facility.

quality and makes precision experiments of various kind possible [6–8]. The ion beam in the ESR is circulating at relativistic ion velocities. To reach even higher precision and to investigate features that are not accessible using a relativistic ion beam, the HCI must be available at very low energy. The final energy shall be below a few keV total energy, with an energy spread smaller than 1 eV. For this purpose, the decelerator-cooler facility, called HITRAP, has been designed and is now under construction at GSI. The produced HCI will first be electron cooled and decelerated in the ESR from 400 MeV/u to an energy of 4 MeV/u. After ejection from the ESR, the ions are further decelerated by a combination of an inter-digital H-type drift tube structure (IH) and a radio-frequency quadrupole structure (RFQ) and injected into a Penning trap. There, the ions are accumulated and cooled to 4 K before they are distributed to the various experiments (see Fig. 1).

In addition to HCI of stable nuclei, those of radioactive nuclei will become available. Radionuclides are produced and separated by use of the fragment separator (FRS) [9] and then injected into the ESR. In the more distant future, HITRAP will be part of the Facility for Low Energy Antiproton and Ion Research (FLAIR) at the planned international accelerator Facility for Antiproton and Ion Research (FAIR). There, HITRAP will not only provide highly charged, stable and radioactive ions at low-energy, but also low-energy antiprotons.

2. Precision experiments with single ions

Precision measurements of basic quantities have been conducted successfully using not only light, but highly charged ions as well. Examples are the electronic g -factor, the binding energy of electrons, and the atomic mass. The electronic g -factor of hydrogen-like ions can be used to test the theory of quantum electrodynamics in strong fields. In turn, fundamental constants like the electron mass or the fine-structure constant α can be determined by these measurements if the results of reliable quantum electrodynamics calculations are used as input [10]. The mass of HCI is another important quantity. A determination of the mass of the ion in different charge states gives a new access to the binding energy of the inner electrons. The atomic mass, measured for different nuclei, reveals nuclear binding effects with high precision.

2.1. The g -factor of the bound electron

The g -factor measurement is based on the continuous Stern-Gerlach effect [11] where the g -factor of the bound electron:

$$g = 2 \frac{\omega_L}{\omega_c} \frac{m_e q}{M_{\text{ion}} e} \quad (1)$$

is determined by the ratio of the Larmor frequency ω_L of the electron to the cyclotron frequency ω_c of the ion [12,13]. Additional quantities needed are the ion mass M_{ion} , its charge state q and the mass m_e and charge e of the electron. Remarkable precision can be reached, since the frequency of the oscillations of an ion confined in a Penning trap can be determined with extremely small uncertainty.

If the electronic g -factor of the bound electron can be calculated reliably to a precision that matches that of the experiment, then the electron mass can be extracted from Eq. (1). Using the g -factor measurements of O^{7+} and C^{5+} ions [14,15] the electron mass has been obtained with a four-fold smaller uncertainty [16]. If these measurements can be extended to heavier ions and the QED calculations can be further improved, then the fine structure constant α can be determined in a way completely independent from present procedures [10].

2.2. Mass measurements

Some of the most precise mass measurements have been performed using HCI [17] in a Penning trap. In a Penning trap, charged particles are stored using a combination of a homogeneous magnetic field and a quadrupolar electric field. The motion of the particle can be described by three characteristic parts: the axial oscillation in the electric field with the frequency ν_z and two radial oscillations. These are the gyration of the particle in the magnetic field modified by the electric field, the reduced cyclotron motion with ν_+ , and the $\vec{E} \times \vec{B}$ drift, the magnetron motion with ν_- . The motional frequencies are connected with the free cyclotron frequency:

$$\nu_c = \frac{1}{2\pi} \frac{q}{M} B. \quad (2)$$

via the exact relation:

$$\nu_c = \nu_- + \nu_+ \quad (3)$$

or the invariance theorem [12]:

$$\nu_c^2 = \nu_-^2 + \nu_+^2 + \nu_z^2, \quad (4)$$

which is largely independent on misalignment and distortions of the shape of the electrode. These equations can be used to determine the mass M of the stored particle by connecting measurable frequencies of particles stored in a Penning trap to the cyclotron frequency of particles moving in free space in a homogeneous magnetic field. The magnetic field strength B is usually determined via an ion with a well-known mass like a carbon cluster ion.

The mass resolving power:

$$R = \frac{m}{\Delta m} = \frac{\nu_c}{\Delta \nu_c} \quad (5)$$

determines the precision that can be reached [18]. Combining Eqs. (2) and (5) it is evident that the achievable statistical uncertainty is proportional to the charge state of the probed ion.

The pioneering experiment for mass measurements on HCI [17] reaches a relative mass uncertainty of about 10^{-10} by use of a trap at room temperature and a destructive detection technique. Mass measurements with a precision of 2×10^{-11} have been performed with singly charged ions in a cryogenic Penning trap [19]. Here, the motion of only a single ion stored in the trap has been detected directly and non-destructively. Combining both methods – as possible at HITRAP – will push the relative mass uncertainty even below 1×10^{-11} .

Hence, it will be possible to measure the mass differences between bare and H-like and He-like uranium ions, etc., with an uncertainty below 2 eV. Such measurements would provide the best and direct measurement of the 1s Lamb shift in hydrogen-like heavy ions and provide a stringent test of atomic theory including electron–electron correlations in strong fields. Furthermore, the possibility to produce radioactive nuclei using the FRS will enable for the first time mass measurements with such high precision on radioactive nuclei. These measurements are limited by the half-life of the nucleus of interest because the cooling and preparation will take about 10 s. Hence, the half-life of the isotope under investigation should be at least in the range of 10 s.

3. Other key experiments with slow, highly charged ions

Atomic collisions at low energy provide valuable and indispensable data for many areas of physics, e.g., plasma physics, accelerator physics, and astrophysics. Atomic structure and collision dynamics can be studied by kinematically complete collision experiments using the COLTRIMS technique [20,21]. For HCI, charge exchange is the dominating process at energies of less than a few keV/u. Single or multi-electron capture occurs into high-lying states of the highly charged ion which forms strongly inverted systems, so-called hollow atoms. The initial capture process as well as the de-excitation via X-rays or Auger electrons can be monitored in detail by detecting in coincidence

the recoil ion, the emitted electrons and photons (in the X-ray as well as in the optical spectral region) and by determining their energies.

Electron capture processes will be studied with the available beam intensity of about 10^4 HCI per second. For this the beam of HCI is directed onto a target of, for instance, helium atoms in a supersonic jet. The determination of the recoil ion momentum along with the projectile properties gives information about the energy difference between initial and final state, i.e., the Q -value. If performed for different states this enables high-resolution spectroscopy of the HCI energy levels. The presently achieved resolution of 0.7 eV and uncertainties between 3 and 300 meV [22] are already competitive with methods of conventional spectroscopy. In the future, an improved momentum resolution can be envisaged and hence a reduction of the uncertainty towards the sub-meV level.

Highly charged ions can be used to deposit large amounts of potential energy on surfaces. For instance, the potential energy of several hundred keV of a single bare uranium ion is deposited in a very small area of just a few square nanometers. This high energy density leads in general to a highly non-linear response of matter. For experiments it is, however, important to distinguish between processes induced by the potential energy of the ion due to the high charge state and those induced by kinetic energy. This requires well-defined beams of very low kinetic energy and very small energy spread.

The measured quantity is the number of electrons emitted from the surface during the collision. If this is investigated for different charge states information can be gained on the non-linear response of semi-conductors and insulators to strong Coulomb fields and on defect-induced mobility in the limit of high defect density. The main parameter is the speed at which the insulating material can replenish electrons in the nanometer-sized impact region. A wide range of semi conducting and insulating surfaces produced by thin-film coating shall be studied using this method. In first experiments ions in low charge states were impinging on thin films of LiF [23] and C_{60} [24] evaporated on Au. These experiments indicate that electron spectra depend strongly on the properties of the thin film.

For a certain range of kinetic energies, it might happen that the impinging ion is repelled from the surface without a direct binary collision. This so-called trampoline effect occurs because the positive charges, created on the surface by the first electrons transferred to the incoming ion, are not compensated fast enough. So far experimental evidence for this effect could not be found [25]. Up to now the experimental search was limited by the low charge states available and the large energy spread for beams of only a few eV. Both restrictions will be eliminated by use of the low-energy beam available at HITRAP.

Generally, electronic transitions in HCI are in the far ultraviolet or X-ray spectral range, beyond the access by laser light in the visible spectral region. For very highly charged ions, for instance hydrogen-like ^{207}Pb , the ground-state hyperfine transition (21 cm microwave radiation for atomic hydrogen) is moved into the spectral region accessible by conventional lasers. Since also the lifetime of these states (proportional to Z^{-9}) lies in the microsecond or millisecond range, laser spectroscopy can be

performed with high precision. In this way, the magnetic sector of high-field QED can be tested and – if successfully done – the distribution of the nuclear magnetization can be extracted.

At the HITRAP facility, laser spectroscopy will be performed in a cryogenic environment using a Penning trap kept at 4 K. This offers several advantages: The ions are stored as a dense and well localized cloud (up to 100 000 ions stored within a few cubic millimeters) enhancing this way the overlap with the laser beam. Due to the low temperature the resonance is barely Doppler broadened. In combination with easily achievable high collection efficiency for the fluorescence photons, these properties will allow for an excellent signal-to-noise ratio. Furthermore, the long storage time enables one to optically pump the ions even using the rather weak M1 transition and to reach a high degree of electronic and nuclear polarization.

4. The planned HITRAP facility

An overview of the planned facility is presented in Fig. 1. After production the ions will be decelerated down to 4 MeV/u using the experimental storage ring (ESR) at the present GSI facility. Similarly, at the future FAIR facility the new experimental storage ring (NESR) followed by the low energy storage ring (LSR) will serve to decelerate HCI and antiprotons. The deceleration will be accompanied by electron cooling in the storage ring, such that the emittance of the beam does not grow. Finally, the ions will be collected into a single bunch, extracted from the ESR and injected into a linear decelerator.

4.1. The decelerator

An overview of the linear decelerator and its main components is shown in Fig. 2. The linac structures are pulsed with a maximum duty cycle of 0.5% and 10 Hz repetition rate. The beam extracted from the ESR in a single macro bunch of about 1 μ s length is first re-bunched in a double drift buncher (DDB) [26]. Such, the phase acceptance of the following IH structure, which is typically between 10° and 15° , is extended to accept about 67% of the incoming macro bunch (360° phase spread). The DDB is located 6.1 m in front of the IH structure and uses two cavities separated by a 0.8 m drift at 108 and 216 MHz. Both

cavities are designed as coaxial quarter-wave resonators with four gaps each. The calculated shunt impedance of both cavities is sufficient for providing the required effective gap voltages of 218 and 80 kV respectively by using RF generators with a power of 2 kW.

After re-bunching the beam enters an interdigital H-type (IH) structure and is decelerated to 0.5 MeV/u. The HITRAP IH-structure operates at 108.408 MHz. It has 25 gaps and one triplet inner-tank quadrupole lens and is 2.7 m long. An overall effective voltage of 10.5 MV is required to decelerate ions with a mass-to-charge ratio of 3 to 500 keV/u [27]. The cavity design is optimized in order to reach an effective shunt impedance of 285 M Ω /m. Thus the available GSI power amplifier can be used, which delivers 200 kW rf-peak power. The length of the undercut of the ridges, the ratio of gap-to-drift tube length and the stem thickness has been adjusted for optimal field flatness. The field varies less than 10% within a drift tube section. The two drift tube sections are divided by a 300 mm long section, which contains the magnetic quadrupole triplet lens for transverse focusing and a beam steerer. The required field gradient for the quadrupole lens is 64 T/m and the aperture is 20 mm.

The ion bunch phase spread of $\pm 40^\circ$ behind the IH-structure must be matched to the RFQ acceptance of $\pm 10^\circ$. For this, a two-gap spiral re-buncher will be used in the matching section between IH-structure and RFQ. An existing cavity is being adapted to the HITRAP synchronous particle velocity by changing the drift tubes at the spiral and at the end flanges. At 0.5 MeV/u the cell length and thus the distance between the two gap-center amounts 45.3 mm.

Behind the drift tube structures the ion bunch is injected into a four-rod radio frequency quadrupole (RFQ) resonator to decelerate the ions to an energy of 6 keV/u. The design of the HITRAP four-rod-RFQ is very similar to the 108 MHz structure of the high charge state injector LINAC at GSI [28]. However, the mass to charge ratio used at HITRAP is only three compared to nine at the high charge state injector and permits relaxed rf-power requirements. Therefore only a short structure with an overall length of 1.9 m and a maximum rod voltage of 75 kV is required. The mean aperture radius is about 4 mm, which reduces the peak fields to safe values. To achieve low angular and energy spread, great care has been taken optimizing the rod design. Ad-

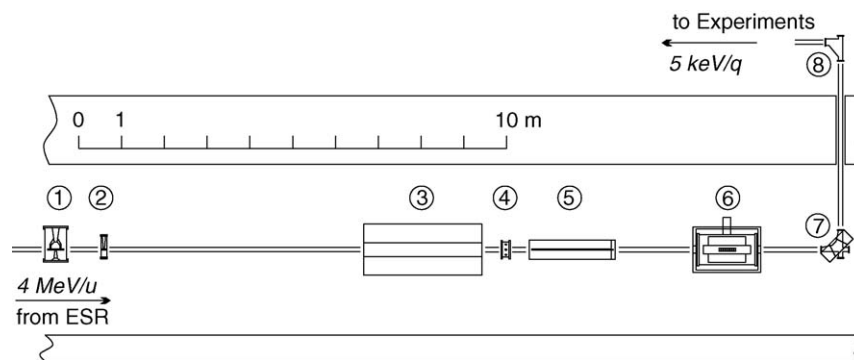


Fig. 2. Side view of the planned HITRAP facility in the reinjection tunnel into the SIS at GSI. The components are: (1) four-gap, 108.408 MHz coaxial buncher; (2) two-gap, 216.816 MHz coaxial buncher; (3) IH-structure; (4) two-gap, 108.408 MHz re-buncher; (5) RFQ and two-gap, 108.408 MHz de-buncher; (6) cooler trap; (7) double focusing bending magnet; (8) spherical electrostatic kicker-bender setup.

ditionally, a two-gap, 108 MHz debuncher is integrated in the RFQ tank to reduce the energy spread. The beam at the exit of the RFQ-debuncher unit has an emittance of 100π mm mrad in both transverse directions and an energy spread of about $\pm 4\%$. This corresponds to a 45% growth of the normalized emittance between the extraction from the ESR and the exit of the RFQ due to non-linearity.

4.2. The low energy beam line and the cooler trap

The low energy beam line connects the radio-frequency quadrupole decelerator with the cooler trap. It provides the differential pumping to separate the extremely good vacuum required for the operation of the cooler trap from the standard high vacuum in the decelerator. Furthermore, the beam diagnosis and matching elements for injection into the strong magnetic field of the trap will be placed in this beam line. Presently the best choice seems to use electrostatic einzel lenses as described in [29].

The cooler trap finally captures the highly charged ions in flight and decreases their phase space volume by electron and resistive cooling. A cylindrical Penning trap in a magnetic field of 6 T is used. The trap will consist of 23 electrodes that can be used to shape the electric potential very flexibly and to create five harmonic trap regions, three for ions and two for electrons.

The first step is the in-flight capture. For this, the ion bunch with a pulse length of about $1 \mu\text{s}$ will be injected into the trapping region and decelerated further from 6 keV/u to approximately 2 keV/u while the ion beam is kept radially small by the strong magnetic field. The incoming bunch is reflected at the downstream trapping electrode and trapped by switching the upstream trapping electrode from the initial potential of ≈ 11 kV to about 18 kV just after injection of the ion bunch. The switching has to be performed within less than 400 ns. Additionally, consecutive ion bunches might be stacked without intermediate cooling. For this, the potential of the inner trap region is lowered in a first step by at least 2 kV, corresponding to the energy spread of the ion bunch, to about 9 kV. The kinetic energy of the ions that are already in the trap is not affected. Hence, the upstream trapping electrode can be opened again for the incoming beam applying 11 kV without losing the ions that are already in the trap, which is on 9 kV. Another pulse can now be caught in-flight. This scheme can be repeated as long as the range of the power supplies is not exceeded. About four consecutive ion bunches might be stacked this way at HITRAP with the projected power supplies.

Then the HCI interact and thermalize with the simultaneously stored electrons. The electrons have a kinetic energy corresponding to 4 K since they emit synchrotron radiation during their storage in a high magnetic field and hence are in equilibrium with the surrounding. However, during thermalization they will be heated and such the final energy after electron cooling is a few electron volt. Since dielectronic recombination is not possible for bare ions and the electron densities are still too low for three-body recombination processes, only radiative recombination must be taken into account. Calculations show that more than 90% of the bare uranium ions sent initially into the trap

remain in the original charge state within the projected cooling time of a few seconds [30,31].

After separation of electron and ion clouds the ions will be cooled further using resistive cooling. The ion cloud oscillating in the Penning trap induces image charges and hence an image current in the trap electrodes. If this signal is fed into a resonant circuit kept at 4 K, the signal will be damped in the circuit and consequently the ion motion is damped until it is in equilibrium with the environment of the circuit [13].

Two modes of extracting the cooled ion cloud are foreseen: slow extraction and bunched extraction. If extracted in a bunch, the scheme is very similar to existing trap facilities where up to 100 million singly charged ions are extracted in a $15 \mu\text{s}$ pulse [32]. This mode is especially well suited for experiments where the ions need to be recaptured in a trap. In the slow extraction mode the stored ions will be ejected distributed over the 10 s that are available until the next decelerated ion bunch arrives. This mode is for example required by ion-surface interaction experiments in order to avoid detector saturation.

4.3. The vertical beam line and connection to experiments

The layout of the HITRAP low-energy beam line, starting right after the cooler trap, is depicted in Fig. 3. The arrangement of the vacuum components as well as of the ion optical parts is shown. The cooled ions will be extracted from the cooler trap into the beam line with kinetic energies of 5 kV per charge unit, either continuously or in pulses with a duration of about $1 \mu\text{s}$. Predetermined by the given locality, the 100 mm diameter beam line leads from the re-injection channel up to a platform on top of the re-injection channel, 5.6 m above the ground floor level, where the experiments will be placed (see Figs. 2 and 3). Thus, the first element in the beam line is a 90° double focusing bending magnet which simultaneously serves as charge state separator. Charge separation is necessary since during the cooling process in the trap, even at optimum technical operation, present model calculations predict that 10–20% of the ions leave the trap with charge states different from their initial one [30,31]. Slits will be placed in the image planes of the double focusing separator magnet, defining the entrance and the exit. A further, electrostatic, 90-degree bender will be installed at the upper end of the vertical beam line, leading the beam to the experiments on the platform. This bender will be a combination of a parallel plate kicker and a bender with spherical electrode. This allows for injection of ions from a test ion source into the experimental beam line for setting up and commissioning.

Electrostatic quadrupole lenses will be used in the 4.85 m long vertical section of the beam line to guide and focus the beam. The quadrupoles might also be used for steering at positions with little space for extra steering electrodes. The small distance between the lenses and the short focal length reduces the distortions of the beam caused by the magnetic field of the earth. For freely drifting $5 \text{ keV}/q \text{ U}^{92+}$ ions a deviation of 1.5 mm per meter and 6 mm over 2 m is expected for a magnetic field component of 0.5 G perpendicular to the beam axis. Calculations with the present optics design including direction and magnitude of

the earth's magnetic field show that a shift of about 1 mm has to be compensated before entering the electrostatic bender.

Beam diagnostic elements, mounted on movable feed-throughs will be installed in the exit image plane of the bending magnet, before the entrance to the electrostatic bender and before the entrance of the beam tube into the concrete shielding to monitor beam current and position. For this, cerium doped YAG crystals and micro-channel plates with phosphorous screens are investigated concerning dynamic range and sensitivity. Typical operating parameters of the HITRAP low-energy beam line after the cooler trap are summarized in Table 1.

All beam line components will be made from ultrahigh vacuum compatible materials, which allow to reach an operating pressure of 10^{-10} mbar after baking the system to 250 °C. In this case the charge exchange rate between ions in the beam and residual gas atoms in the beam tube is estimated to be lower than 0.01% per meter assuming charge exchange cross-sections on the order of 10^{-13} cm² [29]. For the vacuum generation three 125 l/s ion getter pumps are foreseen, distributed along the beam line as shown in Fig. 3. Two getter pumps with a pumping speed of 500 l/s each will be installed at the two 90-degree benders

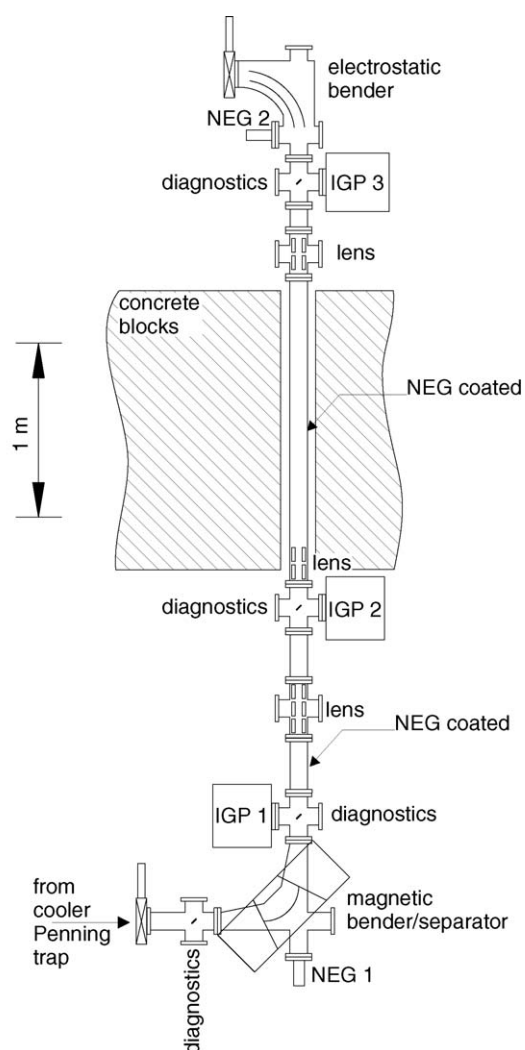


Fig. 3. Sketch of the vertical beam line.

Table 1

The key parameters of the vertical beam line that connects the cooler trap and the experimental setups

Parameter/Element	Value
Beam energy	5 keV/q
Beam intensity	$\leq 10^5$ ions each 10 s
Vacuum	10^{-10} mbar
Separator magnet	
Bending radius	200 mm
Pole shoe gap	25 mm
Typical flux	80 mT
Electrostatic quadrupoles	
Inner diameter	40 mm
Electrode length	80 mm
Typical voltages	± 100 to ± 200 V
Electrostatic bender	
Radius	400 mm
Gap width	30 mm
Typical voltage	375 V

where conductance is bad and the worst pumping conditions are expected according to simulations. Additionally, a 0.5 m long part in the first half of the vertical beam line and a 1.6 m long part in the second half will be coated with a layer of non-evaporable getter (NEG) material to gain additional pumping speed and, simultaneously, to reduce the surface that releases gas. Assuming a pumping speed of about 1 l/s per cm² of NEG material, additional total pumping speeds of 1500 and 5000 l/s can be gained in the respective places for all but rare gases.

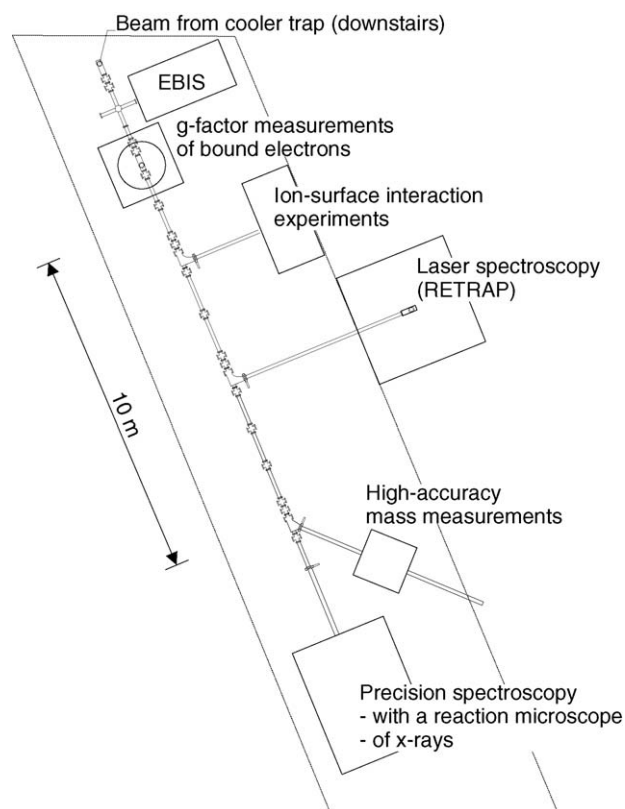


Fig. 4. Sketch of the HITRAP experimental platform on top of the re-injection channel showing the arrangement of the experiments.

A sketch with an arrangement of the different HITRAP experiments on the platform is shown in Fig. 4. For a description of the experiments background refer to Sections 2 and 3.

5. Status

HITRAP is a project to produce and slow down heavy, highly charged ions up to bare uranium. The construction of the major parts of the decelerator has been started in the beginning of 2005. The superconducting magnet for the cooler trap has been ordered mid of 2005. Calls for tender and the orders of the cavities have been placed and delivery is foreseen in 2006. Many of the experimental setups presented in this paper are already prepared and are proceeding with tests using lower charged ions.

HITRAP is also an integral part of the low-energy antiproton and ion facility FLAIR. There the evaluation of the experimental program yielded very positive results for FLAIR and the technical design issues are being worked out.

Acknowledgments

We are very grateful to Jürgen Kluge for promoting and bringing forward this project. Without his enthusiasm, expertise and continuous support its realization would not have been as advanced as it presently is. It was therefore a special pleasure for us to write this article on the occasion of his 65th birthday.

We would like to thank those who contributed to the HITRAP technical design report. Many of the information presented here has been taken from this report. We thank M. Kauschke and C. Welsch for valuable discussions on the cryogenic parts of the trap and the low energy beam line design. We acknowledge furthermore the support by the European Commission under contract number HPRI-CT-2001-50036 (HITRAP) and by the German Ministry for Education and Research (BMBF).

References

- [1] T. Udem, A. Huber, B. Gross, J. Reichert, M. Prevedelli, M. Weitz, T.W. Hänsch, *Phys. Rev. Lett.* 79 (1997) 2646.
- [2] T. Beier, *Phys. Rep.* 339 (2000) 79.
- [3] K. Blasche, B. Franzke, in: V. Suller, Ch. Petit-Jean-Genaz (Eds.), *Proceedings of the Fourth European Particle Accelerator Conference*, London, 1994, World Scientific, Singapore, 1994, p. 133.
- [4] J.W. McDonald, R.W. Bauer, D.H. Schneider, *Rev. Sci. Instrum.* 73 (2002) 30.
- [5] B. Franzke, *Nucl. Instrum. Meth. B* 24 (1987) 18.
- [6] A. Gumberidze, T. Stohlker, D. Banas, K. Beckert, P. Beller, H.F. Beyer, F. Bosch, X. Cai, S. Hagmann, C. Kozhuharov, D. Liesen, F. Nolden, X. Ma, P.H. Mokler, A. Orsic-Muthig, M. Steck, D. Sierpowski, S. Tashenov, A. Warczak, Y. Zou, *Phys. Rev. Lett.* 92 (20) (2004) 203004, <http://link.aps.org/abstract/PRL/v92/e203004>.
- [7] A. Gumberidze, T. Stohlker, D. Banas, K. Beckert, P. Beller, H.F. Beyer, F. Bosch, S. Hagmann, C. Kozhuharov, D. Liesen, F. Nolden, X. Ma, P.H. Mokler, M. Steck, D. Sierpowski, S. Tashenov, *Phys. Rev. Lett.* 94 (22) (2005) 223001, <http://link.aps.org/abstract/PRL/v94/e223001>.
- [8] C. Brandau, C. Kozhuharov, A. Muller, W. Shi, S. Schippers, T. Bartsch, S. Bohm, C. Bohme, A. Hoffknecht, H. Knopp, N. Grun, W. Scheid, T. Steih, F. Bosch, B. Franzke, P.H. Mokler, F. Nolden, M. Steck, T. Stohlker, Z. Stachura, *Phys. Rev. Lett.* 91 (7) (2003) 073202, <http://link.aps.org/abstract/PRL/v91/e073202>.
- [9] H. Geissel, P. Armbruster, K.-H. Behr, A. Brünle, K. Burkard, M. Chen, H. Folger, B. Franczak, H. Keller, O. Klepper, B. Langenbeck, F. Nickel, E. Pfeng, M. Pfützner, E. Roeckl, K. Rykaczewski, I. Schall, D. Scharadt, C. Scheidenberger, K.-H. Schmidt, A. Schröter, T. Schwab, K. Sümmerner, M. Weber, G. Münzenberg, T. Brohm, H.-G. Clerc, M. Fauerbach, J.-J. Gaimard, A. Grewe, E. Hanelt, B. Knödler, M. Steiner, B. Voss, J. Weckenmann, C. Ziegler, A. Magel, H. Wollnik, J. Dufour, Y. Fujita, D. Vieira, B. Sherrill, *Nucl. Instrum. Meth. B* 70 (1992) 286.
- [10] T. Beier, H. Häffner, N. Hermanspahn, S. Djekic, H.-J. Kluge, W. Quint, S. Stahl, T. Valenzuela, J. Verdú, G. Werth, *Eur. Phys. J. A* 15 (2002) 41.
- [11] G. Werth, H. Häffner, W. Quint, *Adv. Atom. Mol. Opt. Phys.* 48 (2002) 191.
- [12] L.S. Brown, G. Gabrielse, *Rev. Mod. Phys.* 58 (1986) 233.
- [13] H. Häffner, T. Beier, S. Djekic, N. Hermanspahn, H.-J. Kluge, W. Quint, S. Stahl, J. Verdú, T. Valenzuela, G. Werth, *Eur. Phys. J. D* 22 (2003) 163.
- [14] V.A. Yerokhin, P. Indelicato, V. Shabaev, *Phys. Rev. Lett.* 89 (2002) 143001.
- [15] J. Verdú, S. Djekic, S. Stahl, T. Valenzuela, M. Vogel, G. Werth, T. Beier, H.-J. Kluge, W. Quint, *Phys. Rev. Lett.* 92 (2004) 093002.
- [16] P.J. Mohr, B.N. Taylor, *Rev. Mod. Phys.* 77 (2005) 1.
- [17] I. Bergström, C. Calberg, T. Fritioff, G. Douysset, J. Schönfelder, R. Schuch, *Nucl. Instrum. Meth. A* 487 (2002) 618.
- [18] G. Bollen, *Nucl. Phys. A* 693 (2001) 3.
- [19] M.P. Bradley, J.V. Porto, S. Rainville, J.K. Thompson, D.E. Pritchard, *Phys. Rev. Lett.* 83 (1999) 4510.
- [20] J. Ullrich, R. Moshhammer, R. Dörner, O. Jagutzki, V. Mergel, H. Schmidt-Böcking, L. Spielberger, *J. Phys. B* 30 (1997) 2917.
- [21] R. Dörner, V. Mergel, O. Jagutzki, L. Spielberger, J. Ullrich, R. Moshhammer, H. Schmidt-Böcking, *Phys. Rep.* 330 (2000) 95.
- [22] D. Fischer, B. Feuerstein, R.D. DuBois, R. Moshhammer, J.R.C. López-Urrutia, I. Draganic, H. Lörch, A.N. Perumal, J. Ullrich, *J. Phys. B* 35 (2002) 1369.
- [23] H. Khemliche, T. Schlathöler, R. Hoekstra, R. Morgenstern, S. Schippers, *Phys. Rev. Lett.* 89 (1998) 1219.
- [24] C. Laulhe, R. Hoekstra, S. Hoekstra, H. Khemliche, R. Morgenstern, A. Närmann, T. Schlathöler, *Nucl. Instrum. Meth. B* 157 (1999) 304.
- [25] J.-P. Briand, S. Thuriel, G. Giardino, G. Borsoni, M. Froment, M. Eddrief, C. Sébenne, *Phys. Rev. Lett.* 77 (1996) 1452.
- [26] V.S. Pandit, P.R. Sarma, R.K. Bhandari, in: F. Marti (Ed.), *Proceeding of the Cyclotrons and their Applications 2001*, East Lansing, USA, AIP Conference Proceedings, vol. 600, 2001, p. 452.
- [27] C. Kitegi, U. Ratzinger, S. Minaev, in: *Proceedings of the LINAC 2004*, Lübeck, Germany, GSI, Darmstadt, Germany, 2004, p. 54, <http://bel.gsi.de/linac2004/INDEX.HTML>.
- [28] J. Klabunde, E. Malwitz, J. Friedrich, A. Schempp, in: K. Takata, Y. Yamazaki, K. Nakahara, (Eds.), *Proceedings of the International Linac Conference*, National Laboratory for High Energy Physics (KEK), Tsukuba, Japan, 1994, p. 704.
- [29] F. Herfurth, T. Beier, L. Dahl, S. Eliseev, S. Heinz, O. Kester, H.-J. Kluge, C. Kozhuharov, G. Maero, W. Quint, The HITRAP collaboration, in: Y. Yamazaki, M. Wada (Eds.), *Physics with ultra slow antiproton beams*, AIP Conference Proceedings, vol. 793, 2005, p.278.
- [30] J. Bernard, J. Alonso, T. Beier, M. Block, H.-J.K.S. Djekić, C. Kozhuharov, W. Quint, S. Stahl, T. Valenzuela, J. Verdú, M. Vogel, G. Werth, *Nucl. Instrum. Meth. A* 532 (2004) 224.
- [31] G. Zwicknagel, in: S. Nagaitsev, R.J. Pasquinelli (Eds.), *International Workshop on Beam Cooling and Related Topics*, AIP Conference Proceedings, vol. 821, 2006, p. 513.
- [32] F. Ames, G. Bollen, P. Delahaye, O. Forstner, G. Huber, O. Kester, K. Reisinger, P. Schmidt, *Nucl. Instrum. Meth. A* 538 (2005) 17.